JCTC Journal of Chemical Theory and Computation

Properties of a Method for Performing Adaptive, Multilevel QM Simulations of Complex Chemical Reactions in the Gas-Phase

M. Graham Guthrie,[†] April D. Daigle,[‡] and Michael R. Salazar*,[†]

Department of Chemistry, Union University, 1050 Union University Drive, Jackson, Tennessee 38305 and Department of Chemistry, Dartmouth College, 6128 Burke Laboratory, Hanover, New Hampshire 03755

Received August 24, 2009

Abstract: The properties of a new method of performing molecular dynamic simulations of complex chemical processes are presented. The method is formulated to give a time-dependent, multilevel representation of the total potential that is derived from spatially resolved quantum mechanical regions. An illustrative simulation is performed on a 110 atom system to demonstrate the continuity and energy conserving properties of the method. The effect of a discontinuous total potential upon the kinetic energy of the system is examined. The discontinuities in the magnitude of atomic force vectors due to changing the electronic structure during the simulation are examined as well as the effect that these discontinuities have upon the atomic kinetic energies. The method, while not conserving total energy, does yield canonical (NVT) simulations. The time reversibility property of the simulation with an extremely discontinuous total potential is discussed. The computational scaling associated with the formation of the spatially resolved, time-dependent groups is also investigated.

1. Introduction

Multiscale modeling of chemical processes has gained much popularity as theoreticians begin to move from what can be calculated on the atomic scale and attempt to join these results to give insight into the meso- and macroscopic scale. Often these simulations involve a mixture of a single high-level quantum mechanical (QM) region surrounded by a lower level molecular mechanical (MM) region. These so-called QM/MM simulations have proven enormously successful in studying many different chemical phenomena, and several review articles have recently appeared.[1−15] In particular, biochemical phenomena have proven to be a fruitful venue of application for chemical modeling via QM/MM methods.[1,4−6,8−10,12,16−20] In these QM/MM simulations, the chemical system is broken into differing regions because the QM calculations needed to understand the phenomena in the QM region, if applied to the whole system, would be computationally prohibitive and would be an inefficient use of computer resources, since what happens inside the MM region only affects the QM region in a derivative manner.

Most often QM/MM methodology is formulated in a static manner, where the defined QM region (that may involve as little as a few atoms to multiples of tens of atoms or molecules) is connected to a defined MM region (typically involving orders of magnitude more atoms/molecules as that found in the QM region), and these regions remain fixed during the course of the simulation. Recently, however, time-dependent (or adaptive) partitioning between the QM and MM regions has provided a means of atomic exchange between regions, where the QM and MM regions are free to change as a function of the simulation time.[21−32] This feature is particularly important when studying chemical systems where the phenomena change significantly in time, such as complex reactive systems, solution dynamics, diffusion, and reactions on surfaces. Perhaps the primary difficulty in these dynamically defined QM/MM methods is the significant discontinuties in the total potential (and,

* Corresponding author. E-mail: msalazar@uu.edu.
[†] Union University.
[‡] Dartmouth College.

10.1021/ct900449q
Published on Web 10/30/2009

perhaps, the atomic force field) and the result that the total energy is not a conserved quantity.[21,24−33] The recent adaptive partitioning method of Heyden and Truhlar[22,23] has been uniquely formulated in a manner that is able to make the connection between dynamically resolved QM and MM regions in a way that does not induce discontinuities in the potential energy and forces, which ensures microcanonical (NVE) ensemble simulations that conserve energy, angular, and linear momentum. The method connects the QM and MM zones through a buffer zone that ensures a smooth transition in the potential and atomic forces for atomic passage by means of $2N$ or N additional multilevel calculations of the buffer zone, where N is the number of groups in the buffer zone.

However, the significant discontinuities resulting in the total potential from time-dependent QM/MM methods has been shown not to induce deviations in the simulations themselves.[21,24,29] The reason for this is that the motions of the atoms in the simulation depend on the gradient of the potential (which yields the force field) and not on the potential itself. Thus, in order to have accurate and smooth simulations, the gradients must be continuous between time steps, not the potential. However, a discontinuous potential will not yield the conservation of the total energy (thus, not a microcanonical ensemble). In spite of this, simulations within the canonical ensemble (NVT) may be obtained from time-dependent QM/MM simulations, if the gradients are approximately continuous. Continuous gradients of the potential yield continuity in the kinetic energy and the smooth atomic motions between time steps where there may be a very large discontinuity in the potential.

When considering chemical systems that lend themselves to necessarily being studied by a time-dependent QM/MM methodology, perhaps the most compelling case is that of the simulation of gas-phase complex reactive processes. These complex processes may be spread over 1 000s of individual reactions with 100s of unique chemical species formed during the entire process.[34−39] In addition, the reactive channels have rates that are both temperature and pressure sensitive. Presently, the chemistry associated with these complex reactive processes is obtained through sophisticated methods of mechanistic postulation.[40−42] Mechanisms are postulated and reduced to the smallest number of reactions possible. Rate coefficients for the individual steps are obtained by fitting to experimental data through the design of experiments for the isolation of the individual reactions to obtain the rate coefficients and through the use of transition-state theory and/or molecular dynamics.[43] In this methodology of postulation and solving for the rate coefficients, the simulated dynamics of the chemical system are determined from the kinetics, rather than the reverse.

And that the kinetics determines the dynamics is for sufficient reason, since direct molecular dynamic simulations of these processes are extremely difficult and have only recently been performed through the use of empirical reactive force fields.[44−47] Consider, these systems are composed of individual reactions that may scale between picoseconds to as long as nanoseconds and between whole processes that are on the order of nano to microseconds. Furthermore, because the chemistry involves so many reactive channels, 100s to 1 000s of atoms are needed in order to perform a meaningful simulation. Thus, simulation of these complex reactive gas-phase systems involves multiscale modeling in both time and system size, necessitating a time-dependent QM/MM methodology, if high-level QM calculations are to be used in order to understand these complex reactive processes.

In addition to requiring a time-dependent QM/MM methodology for the simulation of these complex gas-phase reactive processes, these systems further require a multilevel QM description of the potential. This is the case because a single level of QM theory will not be able to cover all the reactive and nonreactive collisional processes sufficiently well. Consider the treatment of a radical reaction at the same level of theory as a bath gas collisional process. A level of theory sufficient for the radical reaction is too high a level for bath gas collisions, and a level appropriate for the bath gas collisional process is insufficient for the radical reaction. Thus, these complex reactive gas-phase processes require a multilevel QM description due to the difficulties in obtaining accurate potentials for the diverse and numerous collisional processes.

One way of mitigating some of the computational difficulties associated with performing direct molecular dynamic simulations of these complex reactive processes has been suggested through the formulation of the total potential into time-dependent, spatially-resolved groups over which multiple levels of electronic structure may be applied.[29] This method allows one to avoid the use of a single level of electronic structure for all interactions within the simulation. Spatially resolved groups are formed during the course of the simulation, and an appropriate level of QM theory is applied to the groups depending on their chemical nature. This time-dependent, multilevel QM methodology allows the use of high levels of electronic structure for demanding reactive collisions, while also allowing use of lower levels of electronic structure for nonreactive collisional processes.

The subject of this work is an examination into the properties of such a time-dependent, multilevel QM molecular dynamics method. The method may be represented as nQM (QM1/QM2/QM3/..., where each QM level is for individual groups). The intergroup (group−group) MM interactions were set to zero for this study. A 110 atom nonreactive simulation is performed in order to examine the continuity properties of this adaptive nQM method. The simulation and levels of theory chosen for the various groups are described in Section II. Section III examines energy continuity and conservation properties that result from a time-dependent, multilevel QM description of the potential. The continuity of the atomic forces is examined in Section IV over two changes in groups where the QM levels describing the groups differ widely. The atomic kinetic energies of the atoms involved in the two groups are also examined. Section V examines the time reversibility of the simulations. The computational scaling associated with the formation of the groups is investigated in Section VI. The conclusions are given in Section VII along with a brief description of the future development of the computational tools in order to

perform direct molecular dynamic simulation of complex reactive processes in the gas-phase.

II. Illustrative Simulation

In order to examine the properties of a time-dependent, multilevel QM molecular dynamics methodology, a 110 atom simulation with 10 ethylene (C_2H_4), 10 carbon dioxide (CO_2), and 10 carbon monoxide (CO) molecules were placed into a cubic simulation cell of size 65 bohr per side and a total volume of 40.70 nm^3. The molecules were randomly placed in the simulation cell and equilibrated at a temperature of 300 K using ReaxFF,[48] giving an ideal pressure of 30.1 atm. After equilibration with ReaxFF, the atomic coordinates and velocities of the system were used as initial conditions for a nonthermostated simulation. For this 110 atom system, individual C_2H_4, CO_2, and CO molecules were treated at MP2/McLean and Chandler (MC), SVWN/6-31G, and RHF/STO-3G levels of theory, respectively. For groups mixed with combinations of molecular systems, the following rules were employed: combinations of molecules containing all three CO, CO_2, and C_2H_4 species, the RHF/STO-3G level of theory was employed; for CO and C_2H_4 only, the SVWN/6-31G level of theory was employed; for any combination of CO_2 and C_2H_4 with fewer than 20 atoms, the MP2/MC level of theory was used; for any combination of CO_2 and C_2H_4 with more than 20 atoms, the RHF/STO-3G level of theory was employed. Although not exhaustive, these rules were sufficient for the simulations reported herein. The 20 atom break was used to ensure that the simulation would not require more memory than available. The GAMESS electronic structure suite of programs was used to calculate the energy and gradients during the course of the simulation.[49] A 3.86 Å (7.30 bohr) diatom spatial cutoff was used to define the groups. Thus, any atom pair within this cutoff will be part of the same group (Section VI has more information on group formation). A larger spatial cutoff will have even better continuity properties than illustrated below.

In addition, the levels of electronic structure and basis sets were specifically chosen to ensure very significant changes in the level of theory used for describing the groups. In fact, it is recognized (and was such designed) that these selections represent poorer choices than would likely be used, resulting in much larger changes in the description of electronic structure when the groups change. Thus, the continuity properties outlined in this work were designed to be closer to the worst-case scenario, rather than the best that can be achieved.

III. Continuity and Conservation Properties

a. Potential and Total Energy. The 110 atom simulation began with a connectivity list given in Table 1 and a total potential energy of $-3.7522050175 \times 10^3$ Hartrees. A time step of 10 au of time (~0.242 fs) was employed for the simulation and Hamilton's 6N first-order equations of motion were solved using a velocity Verlet numerical integrator. Shown in Figure 1 are plots of the total potential energy (*y*-axis) and the energy conservation ($E(t) - E(0)$, secondary *y*-axis) as a function of simulation time, where the total

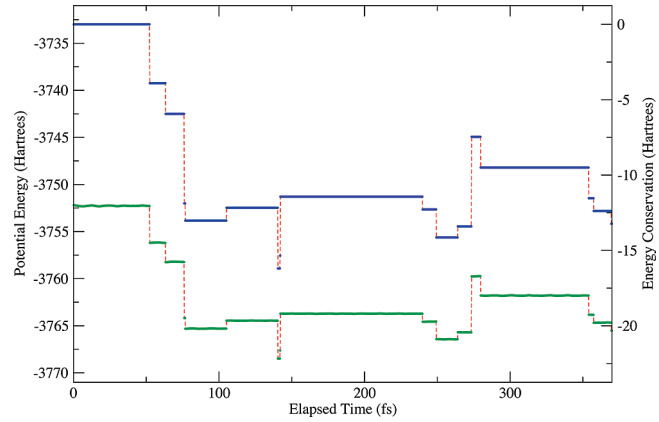

Figure 1. Continuity in the total potential energy (*y*-axis, green circles and red-dashed lines) and the conservation of total energy (secondary *y*-axis, blue circles and red-dashed lines) for an 110 atom simulation.

Table 1. The Groups at the Beginning of the 110 Atom Simulation

group size	number of members	molecules in group	level of theory
2	5	CO	RHF/STO-3G
3	3	CO_2	SVWN/6-31G
5	1	CO, CO_2	RHF/STO-3G
6	4	C_2H_4	MP2/MC
9	2	CO_2, C_2H_4	MP2/MC
11	1	CO, CO_2, C_2H_4	RHF/STO-3G
14	1	CO, 2 CO_2, C_2H_4	RHF/STO-3G
19	1	2 CO, CO_2, 2 C_2H_4	RHF/STO-3G

potential energy is shown as small green circles connected by red-dashed lines and the energy conservation is shown as small blue circles connected by red-dashed lines. This figure shows that the total potential energy begins smoothly with small oscillations in the total potential due to the intragroup interactions (vibrations and internal attractions and repulsions within the initial groups given in Table 1). At a simulation time of 52.5 fs, there is a discontinuous drop in the potential of 3.903 Hartrees, where a CO/CO_2/C_2H_4 11-mer group treated at the RHF/STO-3G level of theory dissociated to a CO/C_2H_4 8-mer plus a CO_2 3-mer, with each product group treated at the SVWN/6-31G level of theory. Continued changes in groups are seen at subsequent times of 63.4, 76.2, 76.9, 105.2, 140.5, 142.0, 142.2, 240.0, 249.4, 264.1, 273.6, 279.9, 354.1, 357.5, 369.4 fs with potential energy changes of −2.037, −5.947, −1.135, +0.848, −4.021, +0.850, +3.917, −0.851, −1.862, +0.733, +5.948, −2.042, −2.036, −0.844, −0.849 hartree, respectively.

In examining the conservation of energy, Figure 1 shows that energy is completely conserved (maximum value of -1.052×10^{-4} Hartrees) until the first change of groups at 52.5 fs where the total potential is discontinuous, resulting in the same discontinuity in the total energy. Also shown in Figure 1 is the result that, because groups are formed on the basis of internuclear spatial cutoffs, sometimes the groups (and, thus, levels of QM theory) change rapidly. This is best illustrated at time steps of 76.2, 140.5, and 142.0 where the groups remained unchanged for only 3, 6, and 1 time step, respectively, resulting in a rapidly changing total potential.

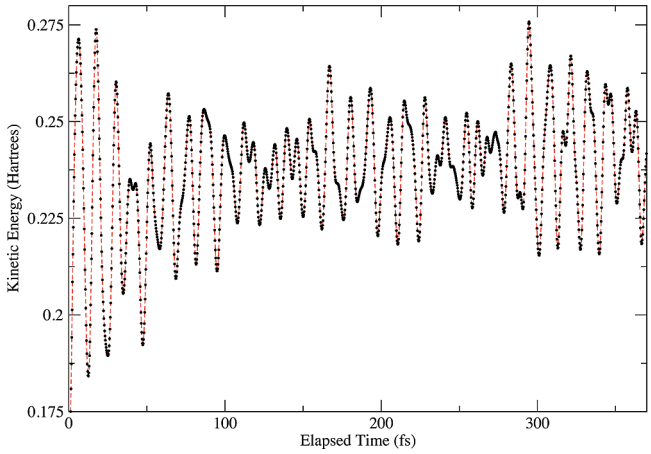

Figure 2. Continuity of the total kinetic energy for 110 atom simulation.

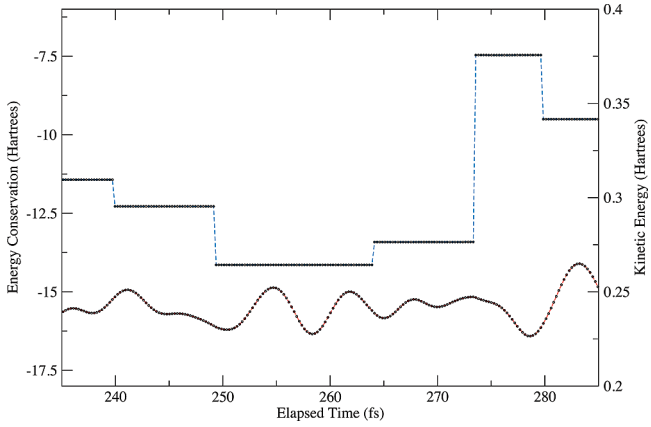

Figure 3. Total energy conservation (black circles connected with blue-dashed line) and continuity of the total kinetic energy (black circles connected by red line) in time window between 235 and 285 fs, where there are five changes in groups.

a. Kinetic Energy. Shown in Figure 2 is a plot of the kinetic energy for the 110 atom simulation of Figure 1 over the same time period. The kinetic energy at each time is shown as small black-filled circles connected by red-dashed lines. This figure shows that, while the total potential undergoes the radical discontinuities seen in Figure 1, the total kinetic energy remains continuous throughout. This is better illustrated in Figure 3, which shows the energy conservation (black circles connected by blue-dashed lines) and the kinetic energy (black circles connected by red-dashed lines) at times between 235 and 285 fs, where there were five changes in the groups and the resulting discontinuity in the total potential. As seen in this figure, the total energy undergoes large discontinuities (of over +5.9 Hartees at $t =$ 273.6 fs), while the kinetic energy is continuous through all these changes, which yields very smooth atomic motions between these extremely large discontinuities in the potential.

To further examine the smoothness of the kinetic energy, the time derivative of the kinetic energy was calculated at each time step within the 235−285 fs simulation window displayed in Figure 3, and these results are shown in Figure 4. The time steps where there was a change in groups and the QM levels of theory used to describe those groups are shown as blue boxes. Figure 4 shows that the gradient of

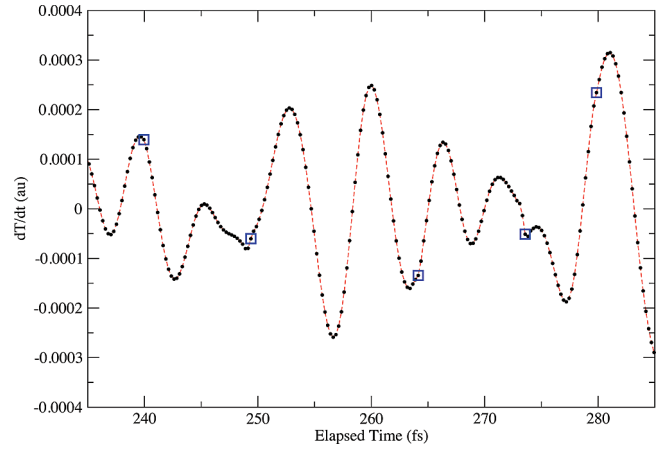

Figure 4. Time derivative of kinetic energy (T) in atomic units in 235−285 fs window. The blue boxes are where there is a change in groups.

the kinetic energy is continuous (C0 continuity), which alone is sufficient for a smooth and continuous kinetic energy. Furthermore, at all times where there was a change in groups and a resulting discontinuity in the total potential, the derivative of the kinetic energy immediately after the change is very smooth, with the possible exception of the point at 273.6 fs where there is a small kink. A similar kink is seen at $t =$ 248.9 fs, where there was not a change in groups. Examining the second time derivative of the kinetic energy (time derivative of Figure 4, not shown) demonstrates that it is discontinuous in this short time window at a few of the times where there is a change in groups ($t =$ 249.4, 264.1, and 273.6 fs). However, the second derivative of the kinetic energy is also discontinuous at times where there are no changes in the groups. The result of this analysis is that continuity of the time derivative of the kinetic energy is sufficient to guarantee a smooth and continuous kinetic energy. Figure 4 shows that this 110 atom simulation has a continuous derivative of the kinetic energy (and, thus, a smooth kinetic energy) when the potential undergoes frequent and significant discontinuities. In addition, the results of Figures 3 and 4 are for a spatial cutoff of 3.86 Å (7.30 bohr). Enlarging the spatial cutoff will improve the smoothness and continuity of the kinetic energy and the gradient of the kinetic energy, respectively.

IV. Atomic Force Continuity

The energy continuity and conservation properties of the 110 atom simulation shown in Figures 1−4 demonstrates that formulating the total potential as time-dependent, multilevel QM groups will result in a radically discontinuous potential with the resulting total energy not being a conserved quantity. However, examining the energy conservation plot of Figures 1 and 3 shows that as long as the groups remain unchanged, the total energy is a conserved quantity. Thus, what is changing with a change in groups is simply the reference total energy, $E(0)$. This is the case because the groups change at spatial cutoffs that are at, or near, the asymptotic region where the gradients of the potential will have approximately the same value, namely zero. Furthermore, the kinetic energy remained continuous despite very significant changes in the

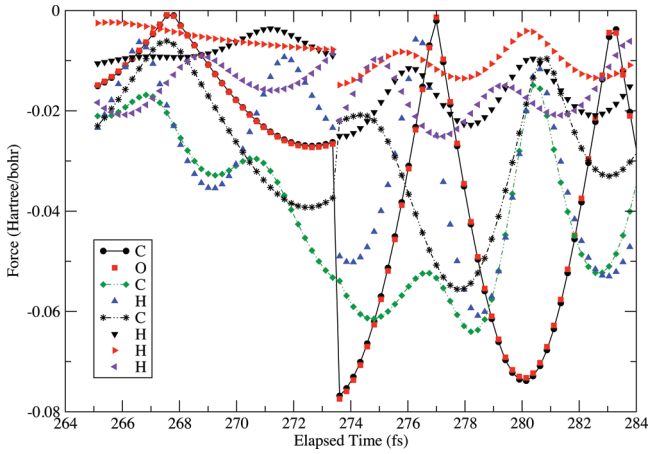

Figure 5. Continuity in the magnitude of the atomic force vectors for 8 of the 14 atoms involved in the change of groups at 273.6 and 279.9 fs.

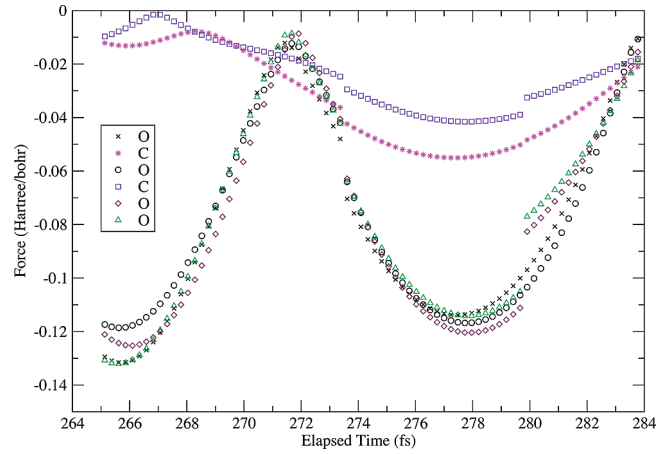

Figure 6. Continuity in the magnitude of the atomic force vectors for the remaining 6 of the 14 atoms involved in the change of groups at 273.6 and 279.9 fs.

level of theory and of basis sets used to describe the intragroup interactions (potentials and forces). During some changes, CO, CO_2, and C_2H_4 molecules went from a low-level RHF/STO-3G to higher levels of theory and larger basis sets of SVWN/6-31G and MP2/MC and vice versa. The levels of theory and basis sets were both chosen to illustrate that even with these large changes in the description of the electronic structure, where local bond distance minima and potential energy profiles will change with the change in levels of electronic structure theory, the kinetic energy remains continuous throughout.

In order to examine the changes in the intragroup atomic forces resulting from changes in QM levels of theory, the magnitude of the atomic force vectors were calculated over the range from 265 to 284 fs, where there were two different changes in groups that involved the same atoms. At 273.6 fs, a $(CO_2)_2$ 6-mer joined a C_2H_4/CO 8-mer to form a 14-mer supermolecule. The 6-, 8-, and 14-mer groups were treated at the MP2/MC, SVWN/6-31G, and RHF/STO-3G levels of theory, respectively. In addition, at 279.9 fs this same $(CO_2)_2/C_2H_4$/CO 14-mer group (RHF/STO-3G) dissociated into a CO_2 3-mer (MP2/MC) and a CO_2/C_2H_4/CO 11-mer (RHF/STO-3G). Shown in Figures 5 and 6 are the magnitude of the atomic force vectors between 265 and 284 fs for all 14 atoms involved in these 2 changes of groups. Lines connect the data for the C atoms in Figure 5 since they are more difficult to follow during this short time window. Figure 5 gives the atomic force vector for the C_2H_4/CO molecules, while Figure 6 gives the atomic force vector for the two CO_2 molecules. The large difference in electronic structure (and in potential energy) at 273.6 fs yielded discontinuities in the magnitude of the atomic force vectors for all atoms except the C atoms (filled green diamonds in Figure 5 and blue squares and purple asterisks in Figure 6). In all these cases, the atoms are going from being treated at a higher level of theory and a larger basis set to a lower level of theory and a very small STO-3G basis set. The subsequent change in groups at 279.9 fs, shown in both Figures 5 and 6, demonstrates that there are no discontinuities in the atomic force vector, except for the CO_2 molecule that leaves the 14-mer group. The atomic force vectors for this

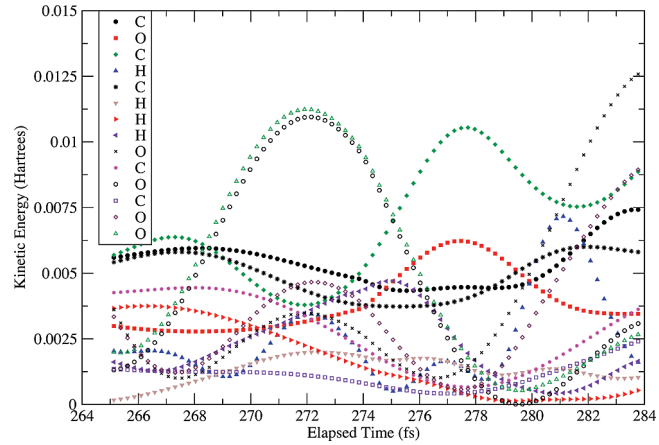

Figure 7. Continuity in the atomic kinetic energies of the 14 atoms involved in the change of groups at 273.6 and 279.9 fs.

CO_2 molecule are the blue squares, green up-facing triangles, and red diamonds in Figure 6. The largest discontinuity in Figures 5 and 6 was at 273.6 fs for the C and O atoms (of the CO molecule), in Figure 5 represented as the black-filled circles and red-filled boxes with a value of −0.0506 hartree/bohr. Thus, Figures 5 and 6 show that significant discontinuities may exist in the gradients of the intragroup potential due to the changes in electronic structure when there is a change in QM levels of theory at the spatial cutoff.

The atomic kinetic energies of the 14 atoms involved in the 2 group changes between 264 and 284 fs are shown in Figure 7. The atoms are given in the same order as shown in Figure 5 and then Figure 6. Although somewhat obscured due to the number of atoms represented in Figure 7, close inspection of the figure shows that, even though there are discontinuities in the magnitude of the atomic force vector at 273.6 and 279.9 fs, all the atomic kinetic energies evolve smoothly through these discontinuities. The kinetic energies of the C and O atoms (black filled circles and red filled boxes, respectively), where there was the largest −0.0506 hartree/bohr discontinuity in the atomic force vectors, also move smoothly through these discontinuities.

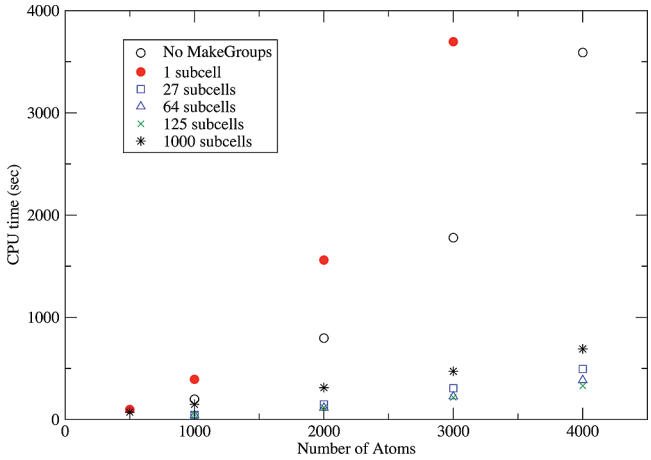

Figure 8. Computational scaling of simulations of N_2 at 300K and ~90 atm pressure with 500 time steps.

In order to examine the effect of a variable spatial cutoff on the discontinuity in the atomic gradients and atomic kinetic energies, single collisions between CO and C_2H_4 molecules were examined. Individual CO and C_2H_4 molecules were treated at the RHF/STO-3G and the MP2/MC levels of theory, while the CO/C_2H_4 supermolecule was treated at the SVWN/6-31G level of theory. Before performing the simulations, the geometries of the individual CO and C_2H_4 molecules were optimized using their respective levels of theory. Seven separate simulations were performed with spatial cutoffs of 4.3−7.3 bohr in increments of 0.5 bohr. The initial geometry of the collisions between the CO and C_2H_4 molecules was at their optimized geometries and at just outside the variable spatial cutoff from one another. The molecules were given center-of-mass velocities to push the molecules together but no internal kinetic energy. The molecules were given no internal kinetic energy in order to examine the effect of the discontinuity in the gradients upon the atomic kinetic energies, and it was not desired to have internal kinetic energy obscure the result. The discontinuity of the magnitude in the atomic force vectors due to the change in the levels of electronic structure was as large as 1.153×10^{-3} Hartrees/bohr, yet resulted in no discontinuities in the atomic kinetic energies across the spatial cutoff. These are precisely the results given above and displayed in Figures 7 and 8, with a spatial cutoff of 7.3 bohr. The difference between spatial cutoffs of 4.3−7.3 bohr is that there is only a very slight acceleration in the atomic velocities after the supermolecule is formed at 7.3 bohr because this spatial cutoff is near the asymptote, where the intermolecular gradients are very close to zero, regardless of the level of theory employed. With a spatial cutoff of 4.3 bohr, these intermolecular interactions are larger, resulting in larger accelerations and decelerations of the center-of-mass velocity vector after the change in levels of theory. Thus, the result of examining a variable spatial cutoff is that kinetic energy is still a continuous quantity, but a spatial cutoff that is too small will lead to sudden accelerations between the molecules, whereas a larger spatial cutoff will give rise to these accelerations in a slower, more physical manner.

V. Time Reversibility

One of the properties of classical molecular dynamic simulations is that they are time reversible. Given a set of initial conditions (atomic coordinates and velocities), one may propagate forward in time, and when the simulation is reversed arrive at the starting point in the exact same number of steps. Time reversibility was examined over the time window of Figure 3, where there are five discontinuities in the potential. The cumulative root-mean-square error (rms) in all the atomic Cartesian coordinates (in Å) at each time between 295 and 235 fs was calculated. The simulation was initialized with the atomic coordinates and the opposite velocities of the 295th fs time step when going forward in time and run for 60 fs using the same time step as before (10 au). This will cause the simulation to go back over the five discontinuities in the opposite direction. The rms error in the atomic coordinates rises slowly and in a very linear manner to reach a maximum value of 3.635×10^{-4} Å after 60 fs, and there is not additional error where there are changes in groups and discontinuities in the total potential. The rms error in the atomic coordinates has a cumulative effect because any deviation in a previous step will be carried through to the next time step. Fitting a slope to the rise in rms error over the 60 fs gives a value of 5.8694×10^{-6} Å/fs for a cumulative rms error of all 110 atomic Cartesian coordinates.

VI. Methodology

The method of performing molecular dynamic simulations by a time-dependent, multilevel QM description of the total potential has been programmed into a suite of programs called **A**ccelerated **Mol**ecular **D**ynamics with **C**hemistry (AMolDC). This multicomponent program divides the total potential into spatially resolved, time-dependent groups where differing levels of electronic structure may be employed over the individual groups in order to place appropriate levels of electronic structure for the various groups formed. Currently, the group−group (intergroup) interactions (MM) have not been implemented but may be computed by low-level QM calculations.

a. MakeGroups. As noted in the 110 atom simulation above, the QM regions are free to change definitions anytime during the simulation, as governed by spatial cutoffs, and it was observed that there may, indeed, be changes in the groups at every time step. Thus, the making of the groups of the simulation will necessarily take place on every time step and will, thus, need to be extremely efficient. In order to accomplish this task efficiently, the simulation cell is broken into link-listed subcells, i.e., each subcell has an explicit link to neighboring subcells. The making of all the groups within the simulation cell proceeds by looping over all the link-listed subcells. Once in a subcell, the groups are formed by looping over all the atoms within the given subcell and by connecting all atoms that are within the spatial cutoff of the atom being looped over. This connectivity list is then looped over to calculate the distance between these and other atoms in the given subcell and in any neighboring subcell, if the atom is within the spatial cutoff of the edge of the

subcell. This process continues until the connectivity list remains unchanged, at which time the process is repeated, being initialized for the next atom in the subcell. After all atoms within the subcell are searched, the next subcell is begun.

The MakeGroups module within AMolDC has been programmed in order to accomplish the task of making the spatially resolved groups at each time step in a simulation. In order to investigate the computational scaling of the MakeGroups module, simulations of N_2 at 300K were performed in which the nitrogens were randomly placed within a simulation cell and propagated for 500 time steps using a simple Morse potential for all internuclear distances. As the number of N_2 molecules was increased, the simulation cell size was adjusted to yield an ideal gas pressure of ~90 atm at 300K. Shown in Figure 8 are the total simulation times without using the MakeGroups module (open circles) and with using the MakeGroups module with 1 subcell (red-filled circles), 27 subcells (open boxes), 64 subcells (open triangles), 125 subcells (×), and 1000 subcells (*). One can see from this figure, the $O(N^2)$ scaling when not using MakeGroups (calculating all interatomic distances) and when using MakeGroups with only 1 subcell (the whole simulation cell). The computational overhead for the MakeGroups module is 1.45 times that of calculating all internuclear distances, as measured by the coefficient of the leading $O(N^2)$ term over the same simulation. However, when the simulation cell is divided into a distribution of 3 × 3 × 3 link-listed subcells, the computational time is greatly reduced, and the computational expense goes from $O(N^2)$ scaling to $O(N)$ scaling. There is little computational difference (relative to the same simulation without MakeGroups) between a 3 × 3 × 3, a 4 × 4 × 4, and a 5 × 5 × 5 division of link-listed subcells. Figure 6 shows that as one continues to increase the number of simulation cells, the computational time becomes more linear. Deviations from linearity come about from the $O(N^2)$ operations of calculating the internuclear distances of the molecules within the individual subcells. Saturation of the simulation cell with subcells, as given most closely by the 10 × 10 × 10 division of link-listed subcells (asterisks), shows almost exactly linear scaling in the number of atoms. Even though the computational cost of MakeGroups is insignificant relative to high-level QM calculations, what is demonstrated in Figure 8 is that, because the total potential is assembled from time-dependent groups, one has the ability to reduce the total number of QM calculations in order to yield overall linear scaling with system size.

VII. Conclusions

The continuity and energy conservation properties of a time-dependent, multilevel QM methodology for the simulation of gas-phase reactive processes have been demonstrated by thoroughly examining a short 110 atom simulation. Although the 110 atom simulation was for nonreactive collisions, a simulation involving reactions will not change the properties illustrated, since all such reactions will be within the asymptotic spatial cutoff. The simulation of reactive processes will call for much higher levels of electronic structure methods to be employed. Simulations of a reactive system are currently being performed.

The principle illustrated in Figures 1−4 is that smooth simulations, within the canonical (NVT) ensemble, result from the framework of a time-dependent, multilevel QM description of the potential that undergoes radical discontinuities over the course of the simulation. However, whenever there is a change in the QM levels of theory, the kinetic energy smoothly traverses these times because the gradients of the potential are all approximately zero at the spatial cutoffs. In addition, Figures 5−7 show that the discontinuities that may result from changes in electronic structure for the intragroup interactions are also shown to not induce discontinuities in the kinetic energy. Thus, smooth atomic motions and continuity in the atomic and cumulative kinetic energy across the boundaries, where there may be significant changes in electronic structure, are also demonstrated.

With a multilevel QM description of the potential that is based on spatially resolved groups, one may place higher levels of theory for those intragroup interactions that demand such treatments (reactive processes) and lower levels of theory for simpler interactions (collisional processes). The AMolDC suite of programs (an nQM method) has been written in order to accomplish these goals. Computational studies show that reducing the total number of potential energy function calls allows the performance of nQM simulations that scale linearly with system size. Future applications will show the utility of a potential energy database (PESDatabase) module in which to store the high-level QM data of the various groups formed during a simulation. These high-level QM data will be used at subsequent simulation times to formulate fast numerical interpolations over the various groups. Thus, an extension in the system size and the simulation time for the direct simulation of complex reactive processes in the gas-phase is performed by the dividing of the total potential into spatially resolved, time-dependent groups over which multiple levels of electronic structures may be employed and the storing of these QM data for subsequent numerical interpolation, once the database is sufficiently populated.

Acknowledgment. Acknowledgment is made to the donors of the American Chemical Society Petroleum Research Fund for support of this research. The authors would like to thank Adri van Duin for helpful conversations and for assistance in using the ReaxFF code.

References

(1) Hao, H.; Weitao, Y. *THEOCHEM* **2009**, *898*, 17.

(2) Zimmer, M. *Coord. Chem. Rev.* **2009**, *253*, 817.

(3) Bernstein, N.; Kermode, J. R.; Csanyi, G. *Rep. Prog. Phys.* **2009**, *72*, 026501.

(4) Kamerlin, S. C. L.; Haranczyk, M.; Warshel, A. *J. Phys. Chem. B* **2009**, *113*, 1253.

(5) Senn, H. M.; Thiel, W. *Angew. Chem., Int. Ed.* **2009**, *48*, 1198.

(6) Siegbahn, P. E. M.; Himo, F. *J. Biol. Inorg. Chem.* **2009**, *14*, 643.

(7) Sproviero, E. M.; McEvoy, J. P.; Gascon, J. A.; Brudvig, G. W.; Batista, V. S. *Photosynth. Res.* **2008**, *97*, 91.

(8) Blumberger, J. *Phys. Chem. Chem. Phys.* **2008**, *10*, 5651.

(9) Hu, H.; Yang, W. *Annu. Rev. Phys. Chem.* **2008**, *59*, 573.

(10) Woods, C. J.; Mulholland, A. J. *Chem. Modell.* **2008**, *5*, 13.

(11) Bo, C.; Maeras, F. *Dalton Trans.* **2008**, *22*, 2911.

(12) Sherwood, P.; Brooks, B. R.; Sansom, M. S. P. *Curr. Opin. Struct. Biol.* **2008**, *18*, 630.

(13) Takahashi, H.; Matubayasi, N.; Nakano, M. *Trends Phys. Chem.* **2007**, *12*, 59.

(14) Senn, H.; Thiel, W. *Top. Curr. Chem.* **2007**, *268*, 173.

(15) Lin, H.; Truhlar, D. G. *Theor. Chem. Acc.* **2007**, *117*, 185.

(16) Takahashi, H. *Front. Biosci.* **2009**, *14*, 1745.

(17) Miani, A.; Helfand, M. S.; Raugei, S. *J. Chem. Theory and Comput.* **2009**, *5*, 2158.

(18) de Visser, S. *Biochem. Soc. Trans.* **2009**, *37*, 373.

(19) Lodola, A.; Mor, M.; Siriak, J.; Mulholland, A. *Biochem. Soc. Trans.* **2009**, *37*, 363.

(20) Dybala-Defratyka, A.; Rostkowski, M.; Paneth, P. *Arch. Biochem. Biophys.* **2008**, *474*, 274.

(21) Bulo, R. E.; Ensing, B.; Sikkema, J.; Visscher, L. *J. Chem. Theory Comput.* **2009**, *5*, 2212.

(22) Heyden, A.; Truhlar, D. G. *J. Chem. Theory Comput.* **2008**, *4*, 217.

(23) Heyden, A.; Lin, H.; Truhlar, D. G. *J. Phys. Chem. B* **2007**, *111*, 2231.

(24) Dongwook, K.; Schatz, G. C. *J. Phys. Chem. A* **2007**, *111*, 5019.

(25) Praprotnik, M.; Kremer, K.; Delle Site, L. *J. Phys. A: Math. Theor.* **2007**, *40*, F281.

(26) Praprotnik, M.; Kremer, K.; Delle Site, L. *Phys. Rev. E: Stat. Phys., Plasmas, Fluids, Relat. Interdiscip. Top.* **2007**, *75*, 17701.

(27) Praprotnik, M.; Delle Site, L. Kremer, K. *Phys. Rev. E: Stat. Phys., Plasmas, Fluids, Relat. Interdiscip. Top.* **2006**, *73*, 66701.

(28) Praprotnik, M.; Delle Site, L.; Kremer, K. *J. Chem. Phys.* **2005**, *123*, 224106.

(29) Salazar, M. R. *J. Phys. Chem. A* **2005**, *109*, 11515.

(30) Hofer, T. S.; Pribil, A. B.; Randolf, B. R.; Rode, B. M. *J. Am. Chem. Soc.* **2005**, *127*, 14231.

(31) Kerdcharoen, T.; Morokuma, K. *Chem. Phys. Lett.* **2002**, *355*, 257.

(32) Kerdcharoen, T.; Liedl, K. R.; Rode, B. M. *Chem. Phys.* **1996**, *211*, 313.

(33) Delle Site, L. *Phys. Rev. E: Stat. Phys., Plasmas, Fluids, Relat. Interdiscip. Top.* **2007**, *76*, 47701.

(34) Pilling, M. J. *Proc. Combust. Inst.* **2009**, *31*, 27.

(35) Slavinskaya, N. A.; Frank, P. *Combust. Flame* **2009**, *156*, 1705.

(36) Blanquart, G.; Pepiot-Desjardins, P.; Pitsch, H. *Combust. Flame* **2009**, *156*, 588.

(37) Taatjes, C. A. *J. Phys. Chem. A* **2006**, *110*, 4299.

(38) Miller, J. A.; Pilling, M. J.; Troe, J. *Proc. Combust. Inst.* **2005**, *30*, 43.

(39) Matheu, D. M.; Dean, A. M.; Grenda, J. M.; Green, W. H. *J. Phys. Chem. A* **2003**, *107*, 8552.

(40) Frenklach, M. *Proc. Combust. Inst.* **2007**, *31*, 125.

(41) Susnow, R. G.; Dean, A. M.; Green, W. H.; Peczak, P. K.; Broadbelt, L. J. *J. Phys. Chem. A* **1997**, *101*, 3731.

(42) Feeley, R.; Frenklach, M.; Onsum, M.; Russi, T.; Arkin, A.; Packard, A. *J. Phys. Chem. A* **2006**, *110*, 6803.

(43) Oran, E. S.; Boris, J. P. In *Numerical Approaches to Combustion Modeling; Progress in Astronautics and Aeronautics Series*, Vol. 135; American Institute of Aeronautics and Astronautics: Washington, DC, 1991.

(44) Chenoweth, K.; van Duin, A. C. T.; Dasgupta, S.; Goddard, W. A. *J. Phys. Chem. A* **2009**, *113*, 1740.

(45) Zhang, L.; van Duin, A. C. T.; Zybin, S. V.; Goddard, W. A. *J. Phys. Chem. B* **2009**, *113*, 10770.

(46) Chenoweth, K.; van Duin, A. C. T.; Goddard, W. A. *J. Phys. Chem. A* **2008**, *112*, 1040.

(47) Strachan, A.; Kober, E. M.; van Duin, A. C. T.; Oxgaard, J.; Goddard, W. A. *J. Chem. Phys.* **2005**, *122*, 54502.

(48) van Duin, A. C. T.; Dasgupta, S.; Lorant, F.; Goddard, W. A. *J. Phys. Chem. A* **2001**, *105*, 9396.

(49) Schmidt, M. W.; Baldridge, K. K.; Boatz, J. A.; Elbert, S. T.; Gordon, M. S.; Jensen, J. H.; Koseki, S.; Matsunaga, N.; Nguyen, K. A.; Su, S.; Windus, T. L.; Dupuis, M.; Montgomery, J. A. *J. Comput. Chem.* **1993**, *14*, 1347.

CT900449Q